Global Journal of Information Technology: Emerging Technologies

Volume 10, Issue 1, (2020) 22-34

www.gjit.eu

Improvement technique of direct torque control of DFIG based in wind energy conversion system

Djamila Cherifi*, GACA Laboratory, Department of Electrical Engineering, University of Dr Moulay Tahar, Saida 20000, Algeria

Yahia Miloud [b], GACA Laboratory, Department of Electrical Engineering, University of Dr Moulay Tahar, Saida 20000, Algeria

Suggested Citation:

Cherifi, D. & Miloud, Y. (2020). Improvement technique of direct torque control of DFIG based in wind energy conversion system. *Global Journal of Information Technology: Emerging Technologies*. *10*(1), 022–034. DOI: 10.18844/gjit.v%vi%i.4630

Received from January 8, 2020; revised from February 10, 2020 ; accepted from 22 April, 2020.
Selection and peer review under responsibility of Prof. Dr. Doğan Ibrahim, Near East University, Cyprus.

Abstract

This article presents a comparative study between two strategies for the direct torque control (DTC) of the doubly fed induction generator based on the wind energy conversion system (WECS). The first method is a conventional DTC and it is based on hysteresis controllers, where the torque and the flux are regulated by these controllers. The second one is DTC by space vector modulation strategy (DTC-SVM), where the torque and flux are regulated by PI controllers. The main feature of the proposed (DTC-SVM) strategy is the reduction of torque and flux ripples. Simulation results of this proposed system were analysed using the MATLAB environment.

Keywords: Doubly fed induction generator (DFIG), wind power generation systems, direct torque control (DTC), space vector modulation (SVM).

* ADDRESS FOR CORRESPONDENCE: **Cherifi Djamila,** GACA Laboratory, University of Dr Moulay Tahar, Saida 20000, Algeria.
E-mail address: d_cherifi@yahoo.fr / Tel.: +213 774864394

1. Introduction

Nowadays, a greater emphasis is given to renewable energies, particularly wind, which is one of the most effective systems available to generate electricity (Sawetsakulanond & Kinnares, 2010). The latest generation wind turbines operate at variable speed. This kind of operation can increase energy efficiency, lower mechanical loads and improve the quality of electrical energy produced. Compared to fixed speed wind turbines, it is the control algorithms that control the active and reactive power produced by the wind turbine at every moment (Cardenas et al., 2009). Currently, the market for wind turbine generators with variable speed has turned to powers greater than 1MW in particular to make the most of the wind farm on the site of implantation. These generators often use the doubly fed induction machine (DFIM) as a generator because of its advantages (Djeriri & Meroufel, 2010; El aimani, Francois, Robyns & Minne, 2003). In fact, the most typical connection diagram of this machine is to connect the stator directly to the network, while the rotor is fed through two static converters in back-to-back mode (one side rotor and the other side network) (Gaillard, Karimi, Poure & Saadate, 2007). This last configuration allows operation of the variable speed wind turbine which gives the possibility of producing the maximum possible power over a wide range of speed variations (± 30% around the speed of synchronism). In addition, the static converters used for the control of this machine can be sized to pass only a fraction of the total power (which represents the power of the slip) (Ghennam & Berkouk, 2010). This implies fewer commutative losses, a lower converter production cost and a reduction in the size of the passive filters, thus reducing costs and additional losses.

In applications requiring significant dynamic performance, a lot of works have been presented with diverse control diagrams of doubly fed induction generator (DFIG). The direct torque control (DTC) was proposed as an alternative to the vector control in the middle of the 1980s by Takahashi (86) and Depenbrock (88) for AC machine controls. This strategy bases on the direct determination of inverter switching states and offers a simpler scheme and less sensitivity to machine parameters. However, the variable switching frequency of DTC causes high flux and torque ripples which lead to an acoustical noise and degrade the performance of the control technique (Ammar, Benakcha & Bourek, 2017; Lazim, Al-khishali Muthanna & Al-Shawi, 2011). With the objective of improving the performance of conventional DTC for the DFIG, in this study, we have developed a technique to reduce torque and flux oscillations by imposing a constant modulation frequency. This technique is called DTC at constant modulation frequency or DTC by space vector modulation (DTC-SVM). Furthermore, this article presents a comparative study between conventional DTC and (DTC-SVM) to control the inverters at two levels to improve the performance characteristics and full efficiency of a wind turbine at variable speed to drive a DFIG. The results of all the discussed aspects of this work have been obtained by numerical simulation using MATLAB/Simulink software.

Nomenclature

DTC	direct torque control
SVM	space vector modulation
DFIG	doubly fed induction generator
WECS	wind energy conversion system

2. Wind turbine conversion system modelling

A wind turbine conversion system is a system that converts the wind turbines mechanical energy obtained from wind into electrical energy through a generator calibrated according to nominal turbine speed, number of generator pole-pairs and network frequency (Bedoud, Mahieddine, Bahi, Lakel & Grid, 2015). Figure 1 shows the synoptic scheme of the studied system.

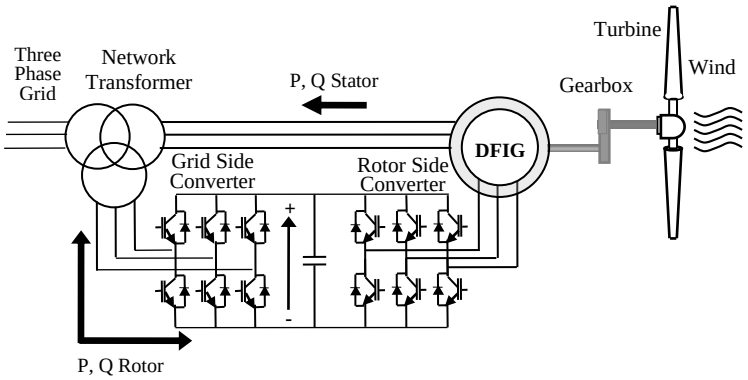

Figure 1. Wind energy conversion chain

The main parts of this scheme are the wind turbine, the gearbox and generator. The rotor-side converter and the grid-side converter connected back-to-back by a dc-link capacitor.

2.1. Turbine modelling

The theoretical power produced by the wind is given by (Barambones, Durana & Kremers, 2013):

$$P_{tur} = C_p \frac{\rho \cdot \mathrm{S} \cdot V_v^3}{2} \tag{1}$$

Where:

C_p represents the wind turbine power conversion efficiency. It is a function of the tip speed ratio λ and the blade pitch angle β in a pitch-controlled wind turbine.

λ is defined as the ratio of the tip speed of the turbine blades to wind speed (Barambones et al., 2013):

$$\lambda = \frac{\mathrm{R} \cdot \Omega_{\mathrm{tur}}}{\mathrm{V_v}} \tag{2}$$

Where R is blade radius. Ω is angular speed of the turbine.

C_p can be described as (Abdeddaim & Betka, 2013):

$$C_p = (0{,}5 - 0{,}0167 \cdot (\beta - 2)) \cdot \sin\left[\frac{\pi(\lambda + 0{,}1)}{18{,}5 - 0{,}3 \cdot (\beta - 2)}\right] - 0{,}0018 \cdot (\lambda - 3)(\beta - 2) \tag{3}$$

The aerodynamic torque expression is given by (Bedoud et al., 2015):

$$T_{tur} = \frac{P_{tur}}{\Omega_{tur}} = C_p \cdot \frac{\rho \cdot \mathrm{S} \cdot V_v^3}{2 \cdot \Omega_{tur}} \tag{4}$$

The gearbox is installed between the turbine and generator to adapt the speed of the turbine to that of the generator (Bedoud et al., 2015):

$$\Omega_{mec} = G.\Omega_{tur} \tag{5}$$

The mechanical equations of the system can be characterised by (Bedoud et al., 2015):

$$T_{mec} - T_{em} = \left(\frac{J_{tur}}{G^2} + J_{gen}\right)\frac{d\Omega_{mec}}{dt} + f_v \cdot \Omega_{mec} \tag{6}$$

2.2. Mathematical modelling of DFIG

In the literature, the Park model of the DFIG is largely used (Kahla, Soufi, Sedraoui & Bechouat, 2015). The equations of voltages for the DFIG stator and rotor in the Park reference frame are given as follows (Zaimeddine & Undeland, 2011):

$$\begin{cases} V_{sd} = R_s i_{sd} + \dfrac{d}{dt}\phi_{sd} - \omega_s \phi_{sq} \\ V_{sq} = R_s i_{sq} + \dfrac{d}{dt}\phi_{sq} + \omega_s \phi_{sd} \end{cases} \tag{7}$$

$$\begin{cases} V_{rd} = R_r i_{rd} + \dfrac{d}{dt}\phi_{rd} - \omega_r \phi_{rq} \\ V_{rq} = R_r i_{rq} + \dfrac{d}{dt}\phi_{rq} + \omega_r \phi_{rd} \end{cases} \tag{8}$$

Where:

The rotor frequency ω_r is given by: $\omega_r = \omega_s - \omega$

ω_s is the electrical pulsation of the stator

ω_r is the rotor one, while ω is the mechanical pulsation of the DFIG.

V_{sd},V_{sq} is the direct and quadrature axis stator voltage

V_{rd}, V_{rq} is the direct and quadrature axis rotor voltage

i_{sd}, i_{sq} is the direct and quadrature axis stator current

i_{rd}, i_{rq} is the direct and quadrature axis rotor current

ϕ_{sd} , ϕ_{sq} is the direct and quadrature axis stator flux

ϕ_{rd} , ϕ_{rq} is the direct and quadrature axis rotor flux

R_s, R_r is the stator and rotor resistance

The flux equations of the DFIG are:

$$\begin{cases} \phi_{sd} = L_s i_{sd} + M i_{rd} \\ \phi_{sq} = L_s i_{sq} + M i_{rq} \end{cases} \tag{9}$$

$$\begin{cases} \phi_{rd} = L_r i_{rd} + M i_{sd} \\ \phi_{rq} = L_r i_{rq} + M i_{sq} \end{cases} \tag{10}$$

L_s, L_r and M are, respectively, the inductance on the stator, the inductance on the rotor and the mutual inductance between two coils.

The electrical model of the DFIG is completed by the following mechanical equation:

$$T_{em} = T_r + f \cdot \Omega + J \cdot \frac{d\Omega}{dt} \tag{11}$$

Here, the electromagnetic torque *Tem* can be written as follows (Ben Amar, Belkacem & Mahni, 2017):

$$T_{em} = \frac{3}{2} p \frac{M}{L_s} \left(\phi_{sq} i_{rd} - \phi_{sd} i_{rq} \right) \tag{12}$$

T_r is the load torque, Ω is the mechanical rotor speed, J is the inertia, f is the viscous friction coefficient and p is the pairs of pole number.

The active and reactive stator and rotor powers are given by (Rao & Laxmi, 2012):

$$\begin{cases} P_s = \frac{3}{2} \left(v_{sd} i_{sd} + v_{sq} i_{sq} \right) \\ Q_s = \frac{3}{2} \left(v_{sq} i_{sd} - v_{sd} i_{sq} \right) \end{cases} \tag{13}$$

$$\begin{cases} P_r = \frac{3}{2} \left(v_{rd} i_{rd} + v_{rq} i_{rq} \right) \\ Q_r = \frac{3}{2} \left(v_{rq} i_{rd} - v_{rd} i_{rq} \right) \end{cases} \tag{14}$$

And the total active and reactive powers of the DFIG are:

$$P = P_s + P_r \tag{15}$$

$$Q = Q_s + Q_r \tag{16}$$

Where positive (negative) values of P and Q mean that the DFIG injects power into (draws power from) the grid (Rao & Laxmi, 2012).

3. Classical DTC principle and scheme for DFIG

DTC achieves a decoupled control of the flux and the electromagnetic torque in the stationary frame (α, β). It uses a switching table for the selection of an appropriate voltage vector. The selection of the switching states is related directly to the variation of the flux and the torque of the machine. Hence, the selection is made by restricting the flux and torque magnitudes within two hysteresis bands. Those controllers ensure a separated regulation of both of these quantities. The inputs of hysteresis controllers are the flux and the torque errors as well as their outputs determine the appropriate voltage vector for each commutation period.

The magnitude of the rotor flux is estimated from its components along the α and β axes (Tamalouzt, Rekioua, Abdessamed & Idjdarene, 2012):

$$\begin{cases} \phi_{r\alpha} = \int_0^t \left(V_{r\alpha} - R_r \, i_{r\alpha} \right) dt \\ \phi_{r\beta} = \int_0^t \left(V_{r\beta} - R_r \, i_{r\beta} \right) dt \end{cases} \tag{17}$$

From these two expressions, we can calculate the rotor flux modulus and the angle δ:

$$\phi_r = \sqrt{\phi_{r\alpha}^2 + \phi_{r\beta}^2} \tag{18}$$

$$\delta = \arctan\left(\frac{\phi_{r\beta}}{\phi_{r\alpha}} \right) \tag{19}$$

The electromagnetic torque can be estimated from the flux estimation and the current measurement using the expression of the torque as a function of the flux and the rotor current given by the following equation:

$$T_{em} = -\frac{3}{2} p\left(\phi_{r\alpha} i_{r\beta} - \phi_{r\beta} i_{r\alpha}\right) \tag{20}$$

3.1. Elaboration of switching tables

The switching table applied in this work is a standard table. This table makes it possible to define the vector which is necessary to apply in each sector starting from the exits of hysteresis regulators (rotor flux and torque) and the position of the rotor flux vector.

The vectors V_0 and V_7 are alternatively selected so as to minimise the number of commutations in the arms of the inverter (Patel & Dyanamina, 2017).

Table 1. Look-up table for inverter voltage vector selection

$\Delta\phi$	ΔT	Sector					
		1	2	3	4	5	6
	1	V_2	V_3	V_4	V_5	V_6	V_1
−1	0	V_0	V_7	V_0	V_7	V_0	V_7
	−1	V_6	V_1	V_2	V_3	V_4	V_5
	1	V_3	V_4	V_5	V_6	V_1	V_2
1	0	V_7	V_0	V_7	V_0	V_7	V_0
	−1	V_5	V_6	V_1	V_2	V_3	V_4

V_0 = [0,0,0]; V_1 = [10,0,0]; V_2 = [1,1,0]; V_3 = [0,1,0]; V_4 = [0,1,1]; V_5 = [0,0,1]; V_6 = [1,0,1]; V_7 = [1,1,1].

Figure 2 shows the block diagram of DTC of DFIG. The stator terminal is connected directly with the grid and rotor terminal is supplied from an inverter. There are two hysteresis control loops, one for the control of torque and the other for the control of flux. The flux controller controls the machine operating flux to maintain the magnitude of the operating flux at the rated value till the rated speed and at a value decided by the field weakening block for speeds above the rated speeds. The torque control loop maintains the torque value to the torque demand.

The output of these controllers together with the instantaneous position of flux vector selects a proper voltage vector. So, it is very important to estimate the rotor flux and machine torque accurately.

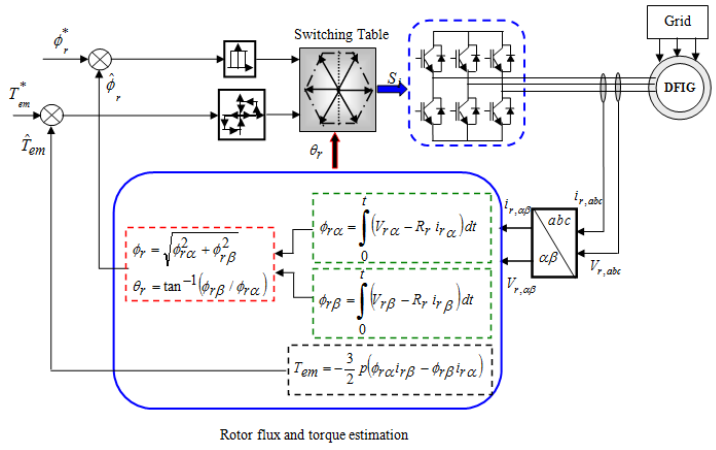

Figure 2. Block diagram of DTC applied to the DFIG

4. Improvement of DTC by technique SVM (DTC-SVM)

The main drawbacks of the conventional DTC are the variable switching frequency and the high level of ripples. Consequently, they lead to high currents harmonics, an acoustical noise and they degrade the control performance. The ripples are affected proportionally by the width of the hysteresis band. However, even with choosing a reduced bandwidth values, the ripples still important due to the discrete nature of the hysteresis controllers. Moreover, the very small values of bandwidths increase inverter switching frequency (Cherifi & Miloud).

The insertion of the space vector modulation (SVM) in DTC control scheme has also been discussed in the literature. SVM preserves a constant switching frequency which can reduce high torque/flux ripples and minimise current harmonic distortion. Consequently, an effective control of the flux and torque is achieved.

This section presents a constant switching frequency DTC strategies based on the torque and flux control in order to improve the classical DTC strategy. This technique uses two (PI) controllers instead of hysteresis controllers to achieve a decoupled control and replaces the switching table by SVM unit for the switching signals calculation.

4.1. Space vector modulation algorithm

This technique is much requested in the field of control in that the reference voltages are given by a global control vector approximated over a modulation period *Tz*. The principle of SVM is the prediction of inverter voltage vector by the projection of the reference vector V_s^* between adjacent vectors corresponding to two non-zero switching states. For two-levels inverter, the switching vectors diagram forms a hexagon divided into six sectors, each one is expanded by 60° as shown in Figure 3.

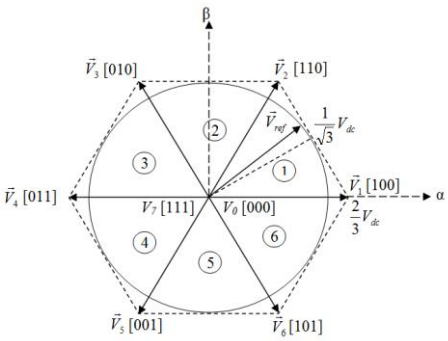

Figure 3. Diagram of voltage space vector

The application time for each vector can be obtained by vector calculations and the rest of the time period will be spent by applying the null vector (Cherifi & Miloud).

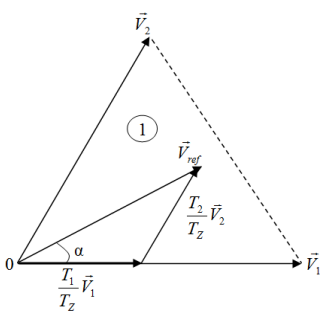

Figure 4. Reference vector as a combination of adjacent vectors at sector 1

When the reference voltage is in sector 1 (Figure 4), it can be synthesised by using the vectors V_1, V_2, and V_0 (zero vector).

The determination of times T_1 and T_2 corresponding to voltage vectors are obtained by simple projections:

$$T_1 = \frac{\sqrt{6}\cdot V_{s\alpha} - \sqrt{2}\cdot V_{s\beta}}{2V_{dc}} T \tag{21}$$

$$T_2 = \frac{\sqrt{2}\cdot V_{s\beta}}{V_{dc}} \cdot T \tag{22}$$

V_{dc}: DC bus voltage.

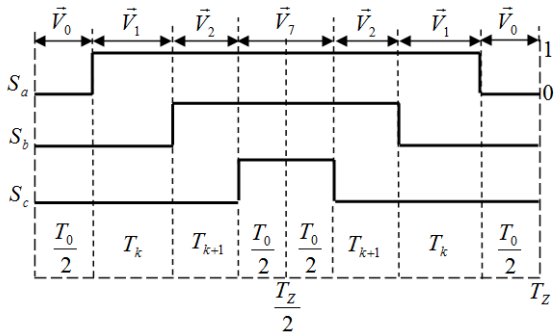

Figure 5. Switching times of sector 1

T_1, T_2 and T_0 are the corresponding application times of the voltage vectors, respectively. T_z is the sampling time.

Figure 6 shows the global block diagram of DTC with SVM.

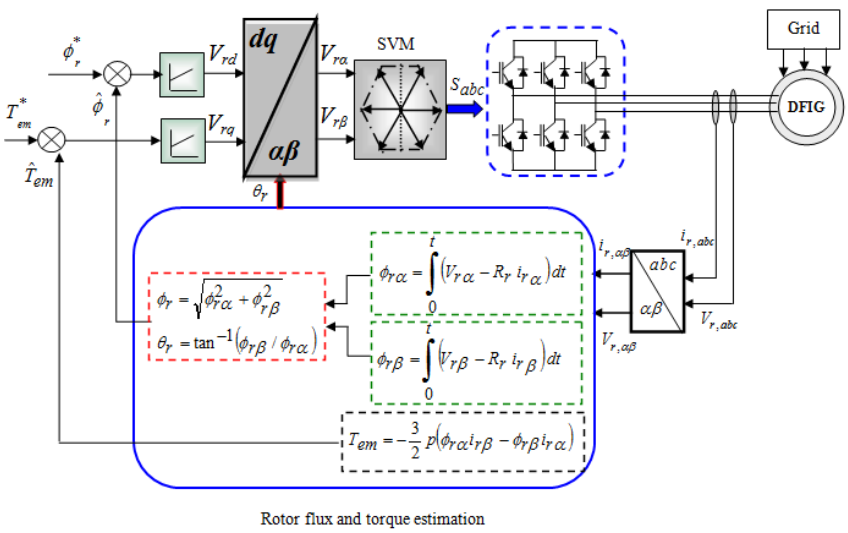

Figure 6. Global control scheme of SVM-DTC with PI controller

5. Simulation results and discussions

In this section, simulations are realised with a 1.5 MW DFIG coupled to a (398V, 50 Hz) network, utilising the MATLAB/Simulink environment. The parameters of the machine are shown in Table 2.

Table 2. Parameters of DFIG

Rated Power Pn	1.5 MW
Stator voltage Vs	398/690 V
Stator frequency f	50 Hz
Stator resistance Rs	0.012 Ω
Rotor resistance Rr	0.021 Ω
Stator inductance L_s	0.0137 H
Rotor inductance L_r	0.0136 H
Mutual inductance M	0.0135 H
Viscous friction *f*	0.0024 Nm/s
Inertia J	1,000 kg m^2
Pairs of poles number P	2

A comparative study between the switching table classical DTC and the DTC with SVM (SVM-DTC) is presented. For the classical DTC (Figure 7), the chosen bandwidths of the hysteresis controllers are ± 0.001Wb for flux and ± 0.7 Nm for torque.

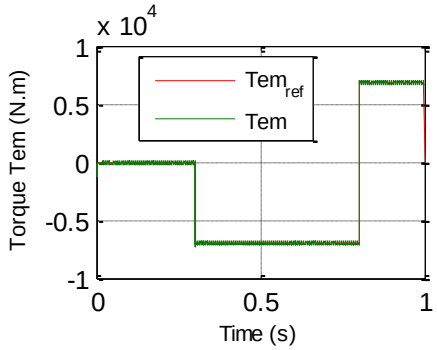

a- Electromagnetic torque

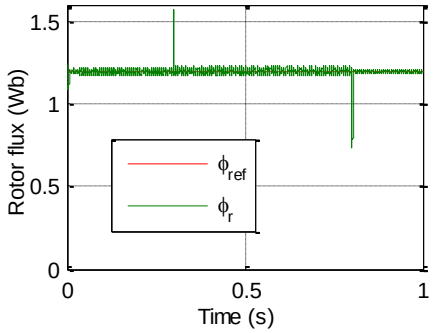

b- Rotor flux

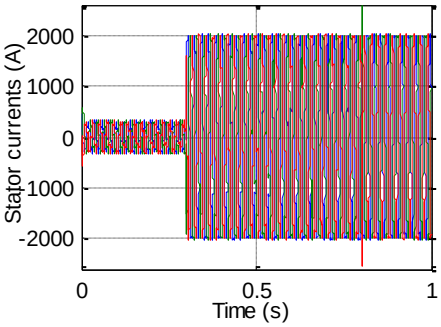

c- Stator currents waveforms

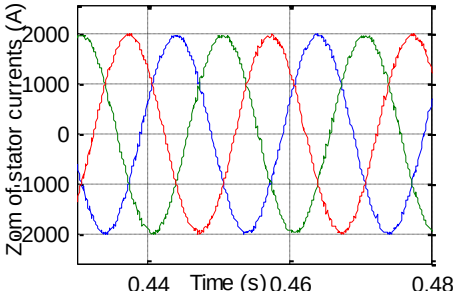

d- Zoom of stator currents waveforms

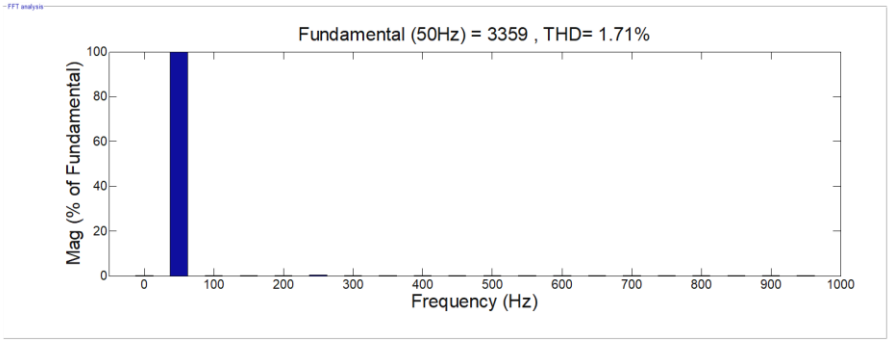

e- Stator current harmonics spectrum

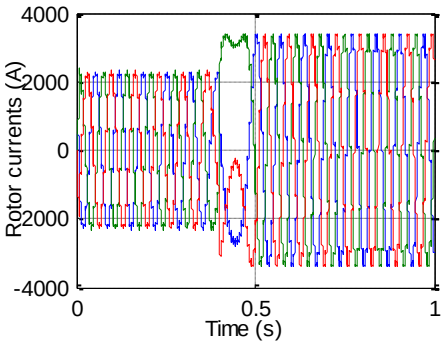

f- Rotor currents waveforms

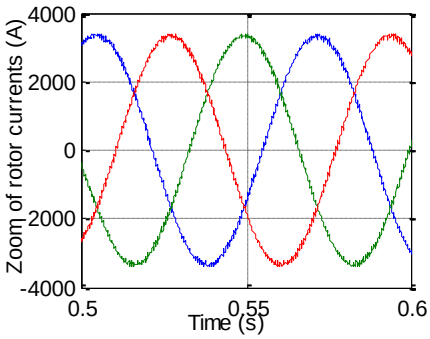

g- Zoom of rotor currents waveforms

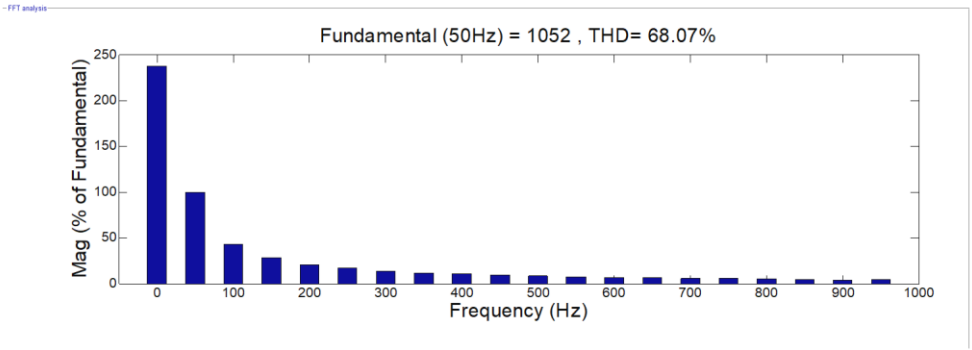

h- Rotor current harmonics spectrum

Figure 7. Simulation performances of conventional DTC of DFIG based on the wind energy conversion system (WECS)

The simulation results of SVM-DTC are shown in Figure 8.

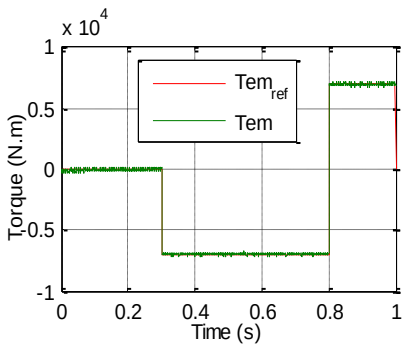

a- Electromagnetic torque

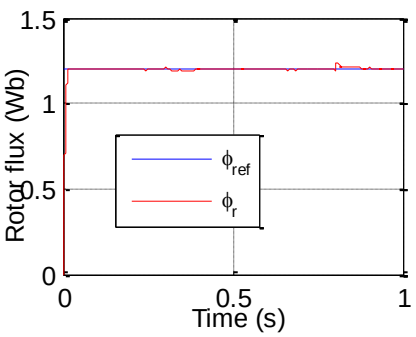

b- Rotor flux

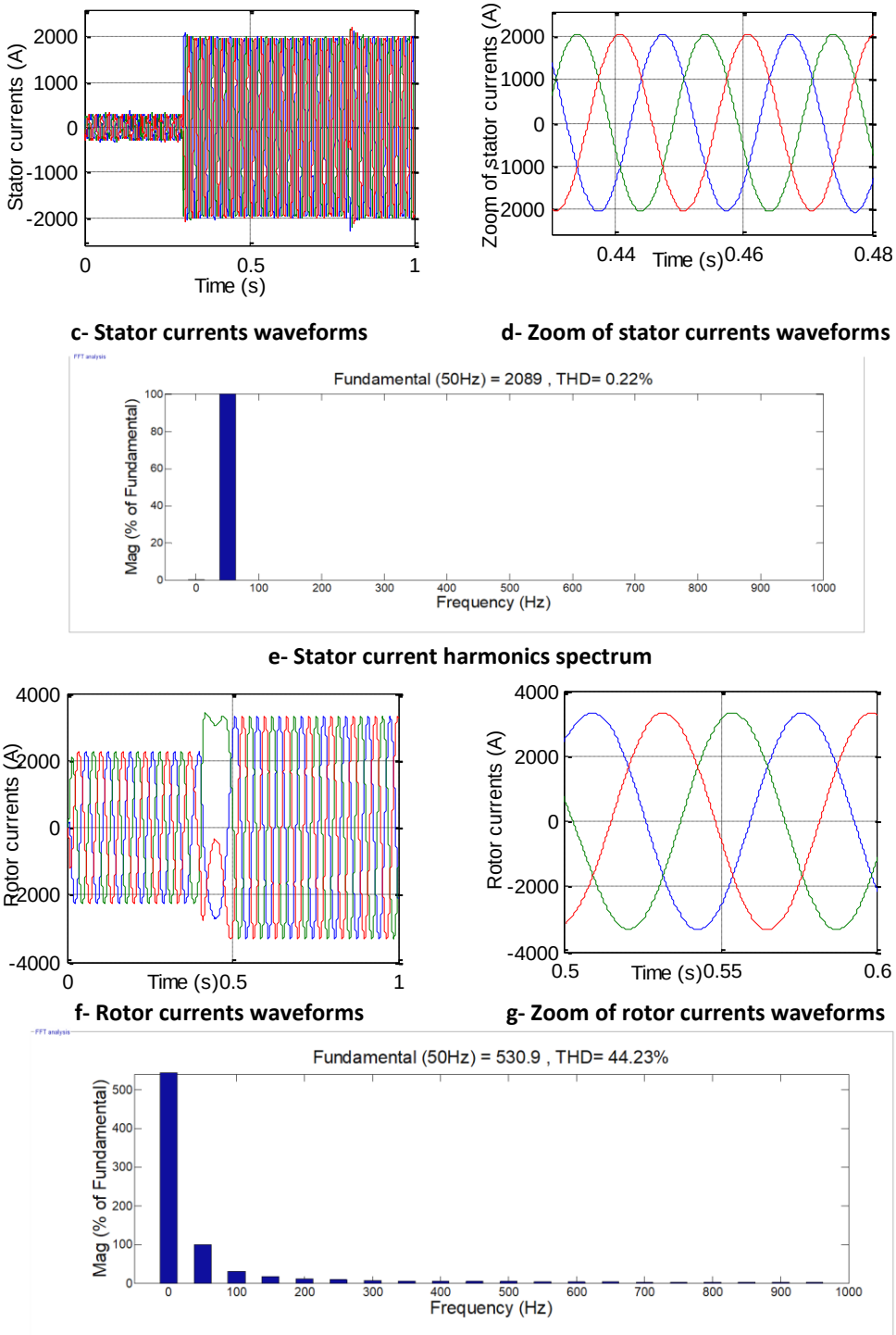

c- Stator currents waveforms

d- Zoom of stator currents waveforms

e- Stator current harmonics spectrum

f- Rotor currents waveforms

g- Zoom of rotor currents waveforms

h- Rotor current harmonics spectrum

Figure 8. Simulation performances of SVM-DTC of DFIG based on WECS

The simulation results of SVM-DTC are shown in Figure 8. We can see from this results, that the flux and torque ripples are significantly reduced compared to the conventional DTC in Figure 7a and b where it is observed that the high torque ripples exceed the hysteresis boundary. Stator and rotor

currents are also presented, the conventional DTC in Figure 7d and g shows a chopped sinusoid waveform of current which indicates to high harmonics level, while SVM-DTC in Figure 8d and g shows a smoother sinusoid waveform.

It is worth-mentioning that the performance of the control is markedly improved with the introduction of the SVM vector modulation.

6. Conclusion

This article presents a comparison study between DTC-SVM and classical DTC. The simulation results obtained for the DTC-SVM illustrate a considerable reduction in torque and flux ripples compared to the classical DTC.

SVM-DTC technique also presents a torque control high performance and dynamic high important while keeping good accuracy of control. This precision is based on the right choice of the voltage vector that plays a role primordial in the regulation of the flux vector therefore torque.

References

Abdeddaim, S. & Betka, A. (2013). Optimal tracking and robust power control of the DFIG wind turbine. *Electrical Power and Energy Systems, 49*, 234–242. doi:10.1016/j.ijepes.2012.12.014

Ammar, A., Benakcha, A. & Bourek, A. (2017). Closed loop torque SVM-DTC based on robust super twisting speed controller for induction motor drive with efficiency optimization. *International Journal of Hydrogen Energy,* 1–13. doi:10.1016/j.ijhydene.2017.04.034

Barambones, O., Durana, J. M. & Kremers, E. (2013). *Adaptive robust control to maximizing the power generation of a variable speed wind turbine*. International Conference on Renewable Energy Research and Applications IEEE, ICRERA; Madrid, Spain, 20–23, October. doi:10.1109/ICRERA.2013.6749745

Bedoud, K., Mahieddine, A., Bahi, T., Lakel, R. & Grid, A. (2015). Robust control of doubly fed induction generator for wind turbine under sub-synchronous operation mode. *Science Direct Energy Procedia, 74*, 886–899. doi:10.1016/j.egypro.2015.07.824

Ben Amar, A., Belkacem, S. & Mahni, T. (2017). Direct torque control of a doubly fed induction generator. *International Journal of Energetica (IJECA), 2*(1).

Cardenas, R., Pena, R., Tobar, G., Clare, J., Wheeler, P. & Asher, G. (2009). Stability analysis of a wind energy conversion system based on a doubly fed induction generator fed by a matrix converter. *IEEE Transaction on Industrial Electronics, 56*(10), 4194–4206. doi:10.1109/TIE.2009.2027923

Cherifi, D. & Miloud, Y. *Direct torque control strategies of induction machine: comparative studies*. London, UK: IntechOpen. doi:10.5772/intechopen.90199

Djeriri, Y. & Meroufel, A. (2010). Field oriented control for doubly fed induction generator using an artificial neural networks dedicated for wind energy conversion systems. International Conference on Power Electronics and Electrical Drives, ICPEED'2010, Oran, Algeria, 26–27 October.

El aimani, S., Francois, B., Robyns, B. & Minne, F. (2003). Modeling and simulation of doubly fed induction generators for variable speed wind turbines integrated in a distribution network. 10th European Conference on Power Electronics and Applications (EPE 2003), Toulouse, France.

Gaillard, A., Karimi, S., Poure, P. & Saadate, S. (2007). Fault tolerant back-to-back converter topology for wind turbine with doubly fed induction generator. *International Review of Electrical Engineering,* 629–636. doi:10.1109/EPE.2007.4417601

Ghennam, T. & Berkouk, E.M. (2010). Back-to-back three-level converter controlled by a novel space-vector hysteresis current control for wind conversion systems. *Electric Power System Research, 10*(5), 444–455. doi:10.1016/j.epsr.2009.10.009

Kahla, S., Soufi, Y., Sedraoui, M. & Bechouat, M. (2015). On-off control based particle swarm optimization for maximum power point tracking of wind turbine equipped by DFIG connected to the grid with energy storage. *International Journal of Hydrogen Energy, 40*, 13749–13758. doi:10.1016/j.ijhydene.2015.05.007

Lazim, M. T., Al-khishali Muthanna, J. M & Al-Shawi, A. (2011). Space vector modulation direct torque speed control of induction motor. *Procedia Computer Science, 5*, 505–512. doi:10.1016/j.procs.2011.07.065

Patel, R. K. & Dyanamina, G. (2017). *Direct torque control of doubly fed induction generator for wind energy conversion system*. IIT-Delhi, India: 8th ICCCNT, July 3–5. doi:10.1109/ICCCNT.2017.8204050

Rao, Y. S. & Laxmi, A. J. (2012). Direct torque control of doubly fed induction generator based wind turbine under voltage DIPS. *International Journal of Advances in Engineering & Technology*.

Sawetsakulanond, B. & Kinnares, B. V. (2010). Design, analysis, and construction of a small scale self-excited induction generator for wind energy application. *Energy Journal, 35*, 4975–4985. doi:10.1016/ j.energy.2010.08.027

Tamalouzt, S., Rekioua, T., Abdessamed, R. & Idjdarene, K. (2012). *Direct torque control of grid connected doubly fed induction generator for the wind energy conversion*. Proceedings of International Renewable Energy Congress IREC'2012, Sousse, Tunisia, pp. 1–6, December 19–22.

Zaimeddine, L. R. & Undeland, T. (2011). Control of a grid connected double-fed induction generator wind turbine. *IEEE Trondheim Power and Technolgy,* 1–7. https://doi.org/10.1109/PTC.2011.6019462